

Photoluminescence study of defect clusters in $\text{Cu}_2\text{ZnSnS}_4$ polycrystals



M. Grossberg*, T. Raadik, J. Raudoja, J. Krustok

Tallinn University of Technology, Ehitajate tee 5, 19086 Tallinn, Estonia

ARTICLE INFO

Article history:

Received 24 September 2013

Received in revised form

16 December 2013

Accepted 31 December 2013

Available online 10 January 2014

Keywords:

Kesterite

$\text{Cu}_2\text{ZnSnS}_4$

Photoluminescence

Defects

ABSTRACT

Temperature dependent photoluminescence (PL) study of $\text{Cu}_2\text{ZnSnS}_4$ (CZTS) polycrystals was performed. The low temperature PL spectrum consists of two PL bands: PL1 at 0.66 eV and PL2 at 1.35 eV. We propose a new radiative recombination model involving theoretically predicted $(\text{Cu}_{\text{Zn}}^- + \text{Sn}_{\text{Zn}}^{2+})$ and $(2\text{Cu}_{\text{Zn}}^- + \text{Sn}_{\text{Zn}}^{2+})$ defect clusters in nearly stoichiometric CZTS. PL1 band at 0.66 eV is proposed to result from a band-to-impurity type recombination related to a deep donor level at 0.66 eV below CBM that originates from the $(\text{Cu}_{\text{Zn}}^- + \text{Sn}_{\text{Zn}}^{2+})$ defect cluster. The PL2 band at 1.35 eV is found to be the dominating radiative recombination path that results from the recombination between electrons and holes in the potential wells caused by the $(2\text{Cu}_{\text{Zn}}^- + \text{Sn}_{\text{Zn}}^{2+})$ clusters that induce a significant band gap decrease of 0.35 eV in CZTS.

© 2014 Elsevier B.V. All rights reserved.

1. Introduction

$\text{Cu}_2\text{ZnSnS}_4$ (CZTS) is considered as non-toxic and low-cost absorber material for solar cells. It has an optimal direct bandgap energy (~ 1.5 eV) for solar energy absorption and high absorption coefficient ($>10^4 \text{ cm}^{-1}$) [1]. The current record of the solar energy conversion efficiency of $\text{Cu}_2\text{ZnSnS}_4$ based solar cells is 8.4% [2], and 11.1% [3] has been obtained with $\text{Cu}_2\text{ZnSn}(\text{S}_x\text{Se}_{1-x})_4$ alloy compound. One prerequisite for obtaining high-efficiency solar cells is the control over the defect structure of the absorber material including electrically active point defects and the presence of secondary phases. Almost all experimental studies on CZTS have shown that this absorber material has a very high point defect concentration. The charged defects are responsible for the spatial potential fluctuations and corresponding characteristic recombination channels. The situation is very similar to the In-rich CuInGaSe_2 (CIGS) absorber material which is today successfully used in thin film solar cells. Usually, at low temperatures band-to-tail (BT) emission dominates in In-rich CIGS and related compounds, in addition, band-to-impurity (BI) and band-to-band (BB) emissions are often observed in the photoluminescence spectra of CIGS compounds [4,5]. However, the situation with CZTS is more complicated. Single broad and asymmetric band around 1.3 eV has been measured in many low-temperature PL studies [6–12]. Our recent paper [6] showed that the PL emission at 1.3 eV in slightly

Cu-rich CZTS polycrystals consists of two PL bands at 1.27 eV and 1.35 eV that both result from BI-recombination. The two bands were attributed to one deep acceptor defect that is present in two different CZTS phases (kesterite and disordered kesterite). The ionization energy of the acceptor defect in both phases was 280 meV. Recently we have also observed [13] band-to-tail (BT) and band-to-band (BB) PL emissions in CZTS at 1.39 eV and 1.53 eV that confirms the applicability of the model of heavily doped semiconductors [14,15] to CZTS. These bands are visible only at room temperature when the dominating PL band at 1.3 eV is quenched. At the same time, the PL band around 1.3 eV with very different thermal quenching properties has also been attributed to donor–acceptor pair recombination [8,9] and free-to-bound recombination [10,11]. In addition, thermal quenching activation energies 48 meV [8], 39 meV and 59 meV [9], 29–40 meV [10], and 140 meV [11] have been previously reported. The different behaviour of the 1.3 eV PL band can be explained by different recombination mechanisms in samples with different chemical composition although the PL emission falls into the same spectral region. According to the theory of heavily doped semiconductors [14] the BI band peak position at low temperature and excitation level is determined as $E_{\text{max}} = E_g - E_T$, where E_T is the thermal activation energy of the related defect. The low temperature bandgap energy E_g of CZTS is reported to be over 1.63 eV [20] and therefore the 1.3 eV PL band with the thermal quenching activation energy lower than about 280 meV must have very different origin and cannot be related to BI emission.

It is known that at high temperatures all charged defects tend to form defect complexes, therefore, the presence of various defect

* Corresponding author. Tel.: +372 6203210.

E-mail addresses: maarja.grossberg@ttu.ee, mgross@staff.ttu.ee (M. Grossberg).

clusters is highly probable. Moreover, it was shown that the formation energies of different defect clusters in CZTS are lower than the formation energies of individual defects [16,17]. Also, in CuInGaSe₂ the $(2V_{\text{Cu}}^- + \text{In}_{\text{Cu}}^{2+})$ complex has very low formation energy, therefore, it plays an important role in the realization of the electronic properties of this absorber [18]. Latest theoretical calculations by Chen et al. [16] predict quite high concentration of $(\text{Cu}_{\text{Zn}}^- + \text{Sn}_{\text{Zn}}^{2+})$ and $(2\text{Cu}_{\text{Zn}}^- + \text{Sn}_{\text{Zn}}^{2+})$ defect clusters in nearly stoichiometric CZTS. The high concentration of these defect clusters will either produce deep recombination centres for electron–hole pairs or cause strong charge carriers trapping. Both mechanisms are detrimental to solar cell parameters. This could be one reason, why the best CZTS solar cell parameters were obtained using Zn-rich materials where the formation probability of these clusters is smaller. Interestingly, according to Chen et al. [16] the detrimental effect of both defect clusters is weaker in quaternary selenide $\text{Cu}_2\text{ZnSnSe}_4$ (CZTSe) since the concentration of these clusters is much lower than in CZTS and the donor levels induced by Sn_{Zn} are shallower in CZTSe than in CZTS. Unfortunately there is no experimental evidence about the presence of these defect clusters in CZTS.

In this paper we implement low temperature PL spectroscopy and present the radiative recombination model for PL emission in CZTS involving $(\text{Cu}_{\text{Zn}}^- + \text{Sn}_{\text{Zn}}^{2+})$ and $(2\text{Cu}_{\text{Zn}}^- + \text{Sn}_{\text{Zn}}^{2+})$ defect clusters.

2. Experimental details

Driven by the theoretical predictions of Chen et al. [16] about the presence of high concentration of defect clusters in nearly stoichiometric $\text{Cu}_2\text{ZnSnS}_4$, a CZTS polycrystalline powder with near stoichiometric composition was synthesized from the binary precursors Cu_2S , ZnS , SnS , and S . The binary precursors and sulphur in amounts corresponding to the stoichiometric composition of CZTS were mixed by grinding in an agate mortar and mounted into a quartz ampoule. The degassed and sealed ampoule with the material was heated at 750 °C for 300 h and then cooled slowly to 200 °C during 300 h. The concentration ratios $\text{Cu}/(\text{Zn} + \text{Sn}) = 0.99$ and $\text{Zn}/\text{Sn} = 0.95$ were obtained for the resulting CZTS polycrystals from EDX analysis. In addition, the presence of ZnS was detected.

For the phase analysis of the samples the room temperature Raman spectra were recorded by using the Horiba's LabRam HR spectrometer equipped with a multichannel CCD detection system in the backscattering configuration. In micro-Raman measurements, the incident laser light with the wavelength of 532 nm was used. The typical Raman spectrum of CZTS presented in Fig. 1, was observed with the peaks at 98, 143, 168, 253, 287, 338, 347, and 368 cm^{-1} . Also, weak signal from ZnS was detected from the

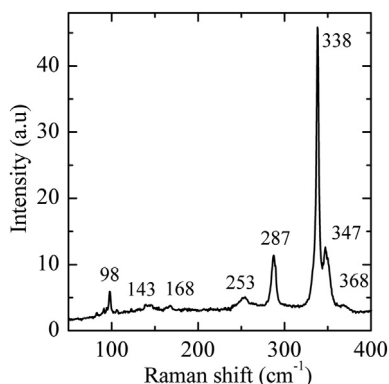


Fig. 1. Raman spectrum of the studied CZTS polycrystals.

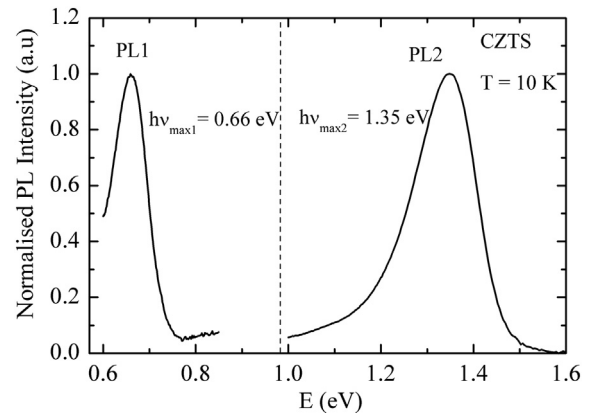


Fig. 2. Low temperature ($T = 10$ K) PL spectrum of CZTS polycrystals. The spectrum consists of two asymmetric PL bands with maxima at 0.66 eV (PL1) and at 1.35 eV (PL2).

polycrystalline powder. For PL measurements, the samples were mounted in the closed-cycle He cryostat and cooled down to 10 K. The 405 nm laser line was used for PL excitation and the spectra were detected by using InGaAs detector.

3. Results and discussion

The low temperature PL spectrum of our CZTS polycrystals with nearly stoichiometric composition is presented in Fig. 2. The spectrum consists of two PL bands: PL1 at 0.66 eV that has not been observed before, and PL2 at 1.35 eV. Both PL bands have asymmetric shape that is typical for semiconductors with high defect concentration [14,15].

In order to determine the recombination mechanism behind the observed PL bands, the temperature and excitation power dependent measurements were performed. The temperature dependencies of the PL bands are presented in Fig. 3. The thermal quenching of the PL1 band was measured in the temperature range of 10 K–180 K and the PL2 band in the temperature range of 10 K–200 K. To eliminate the effect of the background emission and to determine the PL bands parameters such as the peak position and the half-width, all the PL spectra were fitted with empirical asymmetric double sigmoidal function that is proven to be suitable for fitting the typically asymmetric PL bands of the heavily doped semiconductors [4]. The thermal activation energies were determined from the Arrhenius plots (Fig. 4). The linear dependence of $\ln(I)$ versus $1000/T$ at high temperatures was fitted by using theoretical expression for discrete energy levels proposed in Ref. [19]:

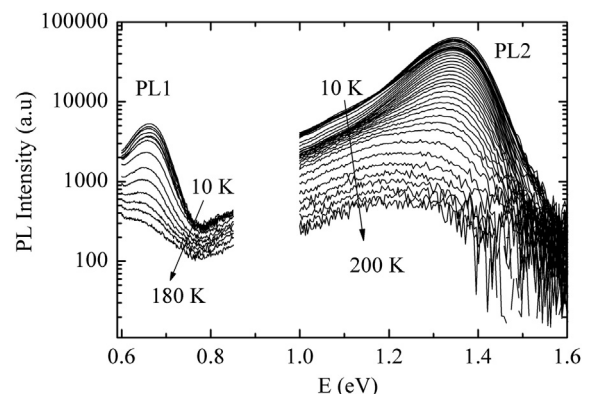


Fig. 3. Temperature dependence of the PL spectra of CZTS polycrystals.

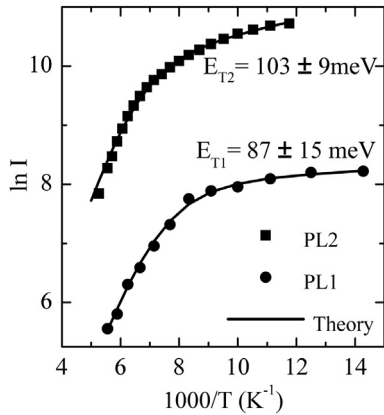


Fig. 4. Arrhenius plots derived from the temperature dependencies of the PL spectra of CZTS polycrystals. Thermal activation energies 87 ± 15 meV and 103 ± 9 meV were obtained for PL1 and PL2, respectively. Solid lines present the fitting of the high temperature experimental data with the theoretical expression (1).

$$I(T) = \frac{I_0}{1 + \alpha_1 T^3 + \alpha_2 T^3 \exp(-E_T/kT)}, \quad (1)$$

where I is integrated intensity, α_1 and α_2 are the process rate parameters and E_T is the thermal activation energy. Activation energies of $E_{T1} = 87 \pm 15$ meV and $E_{T2} = 103 \pm 9$ meV were obtained for PL1 and PL2, respectively. Both PL bands show a shift towards lower energies with increasing temperature (see Fig. 5.) following the temperature dependence of the bandgap energy as found in Ref. [20]. Accordingly, both PL bands show the behaviour similar to BI-band that results from the recombination of a free electron and a hole localised on a deeper defect level, but there is an inconsistency between the PL bands energetic position and the bandgap energy of around 1.64 eV at $T = 10$ K [20]. Interestingly, the PL1 band peak position 0.66 eV is in agreement with the calculated donor energy level position from conduction band minima (CBM) (~ 0.63 eV) for $(Cu_{Zn}^- + Sn_{Zn}^{2+})$ defect cluster [16]. Therefore, we propose that the observed PL1 band results from the recombination involving this donor level. However, this donor level is too deep to be thermally emptied and the thermal activation energy obtained from the thermal quenching of the PL1 band is more likely related to the activation of another non-radiative recombination channel. Alternatively, by assuming that the excited state and the ground state of this defect intersect and we see a phonon assisted quenching that can be treated as an internal quenching, the thermal quenching of

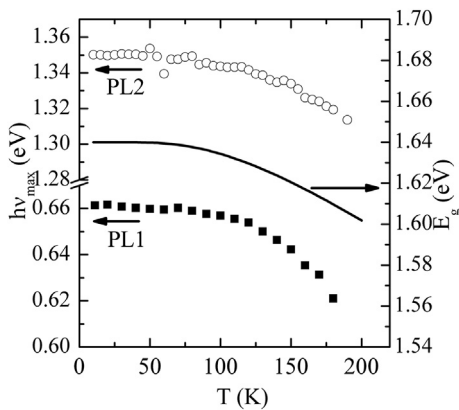


Fig. 5. Temperature dependence of the peak positions of the PL bands presented together with the temperature dependence of the bandgap energy value (solid line) of CZTS as found by Sarswat et al. [20].

the PL1 band can be explained by using the configuration coordinate model [21]. However, it is not possible to differentiate between the two proposed models and the quenching mechanism of this PL band remains unclear.

For the PL2, the thermal activation energy of $E_{T2} = 103 \pm 9$ meV was obtained. As mentioned above, there is an inconsistency between the PL band position and the bandgap energy of CZTS. According to Chen et al. [16] the fully compensated $(2Cu_{Zn}^- + Sn_{Zn}^{2+})$ clusters induce a significant band gap decrease of 0.35 eV that is a sum of CBM red-shift by 0.2 eV and valence band maxima (VBM) upshift of 0.15 eV. As a result, such defect clusters induce deep potential wells for electrons and holes in the material and the recombination between electrons in this conduction band minimum and holes in the valence band maximum is most favourable (see Fig. 6). The thermal activation energy $E_{T2} = 103 \pm 9$ meV determined from the temperature quenching of this PL band is the energy for thermal release of holes from the valence band potential well. Taking into account that the spatial dimension of this kind of potential well induced by the $(2Cu_{Zn}^- + Sn_{Zn}^{2+})$ clusters is in the order of few lattice constants, one can look at it as a quantum well involving discrete states for electrons and holes. These deep wells act as very efficient recombination centres. As a result, BT emission in CZTS has very low intensity and can be detected at 1.39 eV (and the BB band at 1.53 eV) only at high temperatures, when the recombination through wells is quenched [13].

The excitation power dependencies of both PL bands showed a blueshift with increasing laser power with the magnitude of 5 meV/decade for PL1 and 17 meV/decade for PL2. Large blueshift with excitation power is common for heavily doped semiconductors and is predicted by the theory [14,15]. Considering the Raman results that show the presence of disordered kesterite phase in addition to the host material with kesterite crystal structure, one has to take into account the compositional fluctuations leading to the spatially varying bandgap energy of the material. As a result, the maxima of the density of states functions for electrons and holes are broadened that results in the broadening of the PL bands. In addition, different surrounding of the defect clusters may induce local potential fluctuations to the material. From the thermal activation energies determined from the temperature dependencies of the PL bands, one can predict that the density of states function should have a maximum at the energy of the donor state at 0.66 eV below CBM, and at energies corresponding to the maximum of the valence band potential well and minimum of the conduction band potential well. Therefore, the blueshift with excitation power can be explained by the model of heavily doped semiconductors.

Finally, we propose following recombination model (see Fig. 6) for the studied CZTS polycrystals. The dominating radiative recombination mechanism is the recombination between electrons and holes in the potential well caused by the $(2Cu_{Zn}^- + Sn_{Zn}^{2+})$ clusters that induce a significant band gap decrease of 0.35 eV. As a result the PL2 band at 1.35 eV arises. At low temperatures also BI

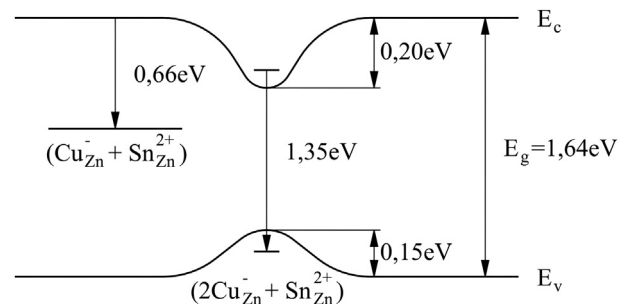


Fig. 6. Radiative recombination model for CZTS polycrystals at $T = 10$ K.

recombination involving deep donor level is present giving the PL1 band with the peak position of 0.66 eV that we propose to originate from the $(\text{Cu}_{\text{Zn}}^- + \text{Sn}_{\text{Zn}}^{2+})$ defect cluster that according to the theoretical calculations [16] is situated ~ 0.63 eV below CBM. Also, the proposed recombination model explains the large energetic distance of the PL bands from the bandgap energy $E_g = 1.64$ eV at $T = 10$ K [20]. In contrast, the dominating PL band in quaternary selenide CZTSe shows the thermal activation energy that corresponds to the energetic distance of the PL band from the bandgap energy [12,22], therefore, the simple BI-recombination model applies to the main PL band in this compound. This can be explained by the smaller probability for the presence of the corresponding defect clusters in CZTSe compared to CZTS as mentioned in the introduction.

4. Conclusion

The photoluminescence study of CZTS polycrystals revealed the presence of $(\text{Cu}_{\text{Zn}}^- + \text{Sn}_{\text{Zn}}^{2+})$ and $(2\text{Cu}_{\text{Zn}}^- + \text{Sn}_{\text{Zn}}^{2+})$ defect clusters. Two PL bands, PL1 at 0.66 eV and PL2 at 1.35 eV were detected at $T = 10$ K. The PL1 band is proposed to result from a BI type recombination related to a deep donor level that originates from the $(\text{Cu}_{\text{Zn}}^- + \text{Sn}_{\text{Zn}}^{2+})$ defect cluster and is located 0.66 eV below CBM. The PL2 is found to be the dominating radiative recombination band that results from the recombination between electrons and holes in the potential wells caused by the $(2\text{Cu}_{\text{Zn}}^- + \text{Sn}_{\text{Zn}}^{2+})$ clusters that induce the significant band gap decrease of 0.35 eV.

Acknowledgement

This work was supported by the Estonian Science Foundation grants G-8282 and ETF 9369, by the target financing by HTM (Estonia) No. SF0140099s08, Estonian Centre of Excellence in Research, Project TK117, and by Estonian Material Technology Programme, Project AR12128.

References

- [1] K. Ito, T. Nakazawa, Electrical and optical properties of stannite-type quaternary semiconductor thin films, *Jpn. J. Appl. Phys.* 27 (1988) 2094–2097.
- [2] B. Shin, O. Gunawan, Y. Zhu, N.A. Bojarczuk, S.J. Chey, S. Guha, Thin film solar cell with 8.4% power conversion efficiency using an earth-abundant $\text{Cu}_2\text{ZnSnS}_4$ absorber, *Prog. Photovoltaics Res. Appl.* 21 (2013) 72–76.

- [3] T.K. Todorov, J. Tang, S. Bag, O. Gunawan, T. Gokmen, Y. Zhu, D.B. Mitzi, Beyond 11% efficiency: characteristics of state-of-the-art $\text{Cu}_2\text{ZnSn}(\text{S,Se})_4$ solar cells, *Adv. Energy Mater.* 3 (2013) 34–38.
- [4] J. Krustok, H. Collan, M. Yakushev, K. Hjelt, The role of spatial potential fluctuations in the shape of the PL bands of multinary semiconductor compounds, *Phys. Scr.* T79 (1999) 179–182.
- [5] M.V. Yakushev, A. Jack, I. Pettigrew, Y. Feofanov, A.V. Mudryi, J. Krustok, Low temperature air-annealing of $\text{Cu}(\text{InGa})\text{Se}_2$ single crystals, *Thin Solid Films* 511–512 (2006) 135–139.
- [6] M. Grossberg, J. Krustok, J. Raudoja, T. Raadik, The role of structural properties on deep defect states in $\text{Cu}_2\text{ZnSnS}_4$ studied by photoluminescence spectroscopy, *Appl. Phys. Lett.* 101 (2012) 102102.
- [7] Hyesun Yoo, JunHo Kim, Lixin Zhang, Sulfurization temperature effects on the growth of $\text{Cu}_2\text{ZnSnS}_4$ thin film, *Curr. Appl. Phys.* 12 (2012) 1052–1057.
- [8] K. Tanaka, Y. Miyamoto, H. Uchiki, K. Nakazawa, H. Araki, Donor-acceptor pair recombination luminescence from $\text{Cu}_2\text{ZnSnS}_4$ bulk single crystals, *Phys. Stat. Sol. A* 203 (2006) 2891–2896.
- [9] Y. Miyamoto, K. Tanaka, M. Oonuki, N. Moritake, H. Uchiki, Optical properties of $\text{Cu}_2\text{ZnSnS}_4$ thin films prepared by sol–gel and sulfurization method, *Jpn. J. Appl. Phys.* 47 (1) (2008) 596–597.
- [10] J.P. Leitao, N.M. Santos, P.A. Fernandes, P.M.P. Salome, A.F. da Cunha, J.C. Gonzalez, G.M. Ribeiro, F.M. Matinaga, Photoluminescence and electrical study of fluctuating potentials in $\text{Cu}_2\text{ZnSnS}_4$ -based thin films, *Phys. Rev. B* 84 (2011) 024120.
- [11] S. Levenco, V.E. Tezlevan, E. Arushanov, S. Schorr, T. Unold, Free-bound luminescence in near stoichiometric $\text{Cu}_2\text{ZnSnS}_4$ single crystals, *Phys. Rev. B* 86 (2012) 045206.
- [12] M. Grossberg, J. Krustok, J. Raudoja, K. Timmo, M. Altsaar, T. Raadik, Photoluminescence and Raman study of $\text{Cu}_2\text{ZnSn}(\text{Se}_x\text{S}_{1-x})_4$ monograins for photovoltaic applications, *Thin Solid Films* 519 (2011) 7403–7406.
- [13] M. Grossberg, P. Salu, J. Raudoja, J. Krustok, J. Photon, Micro-photoluminescence study of $\text{Cu}_2\text{ZnSnS}_4$ polycrystals, *Energy* 3 (1) (2013) 030599.
- [14] A.P. Levanyuk, V.V. Osipov, Edge luminescence of direct-gap semiconductors, *Sov. Phys. Usp.* 24 (1981) 187–215.
- [15] B.I. Shklovskii, A.L. Efros, *Electronic Properties of Doped Semiconductors*, Springer, Berlin Heidelberg New York, 1984.
- [16] Shiyoun Chen, Lin-Wang Wang, Aron Walsh, X.G. Gong, Su-Huai Wei, Abundance of Cu_{Zn} and Sn_{Zn} and $2\text{Cu}_{\text{Zn}} + \text{Sn}_{\text{Zn}}$ defect clusters in kesterite solar cells, *Appl. Phys. Lett.* 101 (2012) 223901.
- [17] S. Chen, J.-H. Yang, X.G. Gong, A. Walsh, S.-H. Wei, Intrinsic point defects and complexes in the quaternary kesterite semiconductor $\text{Cu}_2\text{ZnSnS}_4$, *Phys. Rev. B* 81 (2010) 245204.
- [18] S.B. Zhang, S.-H. Wei, A. Zunger, H. Katayama-Yoshida, Defect physics of the CuInSe_2 chalcopyrite semiconductor, *Phys. Rev. B* 57 (1998) 9642–9656.
- [19] J. Krustok, H. Collan, K. Hjelt, Does the low temperature Arrhenius plot of the photoluminescence intensity in CdTe point towards an erroneous activation energy? *J. Appl. Phys.* 81 (1997) 1442–1445.
- [20] Prashant K. Sarswat, Michael L. Free, A study of energy band gap versus temperature for $\text{Cu}_2\text{ZnSnS}_4$ thin films, *Phys. B* 407 (2012) 108–111.
- [21] J.I. Pankove, *Optical Processes in Semiconductors*, Prentice-Hall, Englewood Cliffs, NJ, 1971.
- [22] M. Grossberg, J. Krustok, K. Timmo, M. Altsaar, Radiative recombination in $\text{Cu}_2\text{ZnSnSe}_4$ monograins studied by photoluminescence spectroscopy, *Thin Solid Films* 517 (2009) 2489–2492.